

Haemodynamic imaging of thoracic stent-grafts by computational fluid dynamics (CFD): presentation of a patient-specific method combining magnetic resonance imaging and numerical simulations

Marco Midulla · Ramiro Moreno · Adil Baali ·
Ming Chau · Anne Negre-Salvayre · Franck Nicoud ·
Jean-Pierre Pruvo · Stephan Haulon · Hervé Rousseau

Received: 28 November 2011 / Revised: 16 February 2012 / Accepted: 22 February 2012
© European Society of Radiology 2012

Abstract

Objectives In the last decade, there was been increasing interest in finding imaging techniques able to provide a functional vascular imaging of the thoracic aorta. The purpose of this paper is to present an imaging method combining magnetic resonance imaging (MRI) and computational fluid

dynamics (CFD) to obtain a patient-specific haemodynamic analysis of patients treated by thoracic endovascular aortic repair (TEVAR).

Methods MRI was used to obtain boundary conditions. MR angiography (MRA) was followed by cardiac-gated cine sequences which covered the whole thoracic aorta. Phase contrast imaging provided the inlet and outlet profiles. A CFD mesh generator was used to model the arterial morphology, and wall movements were imposed according to the cine imaging. CFD runs were processed using the finite volume (FV) method assuming blood as a homogeneous Newtonian fluid.

Results Twenty patients (14 men; mean age 62.2 years) with different aortic lesions were evaluated. Four-dimensional mapping of velocity and wall shear stress were obtained, depicting different patterns of flow (laminar, turbulent, stenosis-like) and local alterations of parietal stress in-stent and along the native aorta.

Conclusions A computational method using a combined approach with MRI appears feasible and seems promising to provide detailed functional analysis of thoracic aorta after stent-graft implantation.

Key Points

- *Functional vascular imaging of the thoracic aorta offers new diagnostic opportunities*
- *CFD can model vascular haemodynamics for clinical aortic problems*
- *Combining CFD with MRI offers patient specific method of aortic analysis*
- *Haemodynamic analysis of stent-grafts could improve clinical management and follow-up.*

Electronic supplementary material The online version of this article (doi:10.1007/s00330-012-2465-7) contains supplementary material, which is available to authorized users.

M. Midulla (✉) · J.-P. Pruvo
Cardiovascular Radiology, University Hospital of Lille,
Lille, France
e-mail: marco.midulla@chru-lille.fr

R. Moreno · H. Rousseau
Radiology, Rangueil University Hospital,
Toulouse, France

F. Nicoud
University Montpellier II – CNRS UMR 5149 I3M, CC 051,
Montpellier, France

S. Haulon
Vascular Surgery, University Hospital of Lille,
Lille, France

M. Chau
ASA, Advanced Solutions Accelerator,
University of Toulouse 3 Paul Sabatier,
Montpellier, France

R. Moreno · A. Baali · A. Negre-Salvayre · H. Rousseau
INSERM/UMR 1048 Cardiovascular and Metabolic
Diseases, University of Toulouse 3 Paul Sabatier,
Toulouse, France

Keywords Time-resolved 3D MRI · CFD · TEVAR · Stent-graft · Haemodynamics

Abbreviations

MRI	Magnetic resonance imaging
CFD	Computational fluid dynamics
TEVAR	Thoracic endovascular aortic repair
MRA	Magnetic resonance angiography
PCI	Phase contrast imaging
WSS	Wall shear stress
BTFE	Balanced turbo field echo
TAA	Thoracic aortic aneurysms
PU	Penetrating ulcers
IMH	Intramural haematoma
ATAR	Acute traumatic aortic rupture

Introduction

In the last decade, thoracic endovascular aortic repair (TEVAR) has become a widespread treatment option for thoracic aortic diseases, finding general acceptance among the medical community as an alternative to surgery [1–3]. Cardiovascular imaging plays a crucial role in treatment planning and patient follow-up: diagnostic findings influence clinical management and are directly related to technical issues such as device selection and sizing. All routinely available techniques certainly provide well-detailed analysis of the aortic morphology but, so far, none of them allows for functional exploration of the post-implantation status of patients treated by TEVAR. More recently, 4D MRI with high-field-intensity machines has been proposed for flow analysis of the thoracic aorta [4, 5], and haemodynamic assessments of different normal and pathological aortic scenarios have been reported [6–8]. The results presented in these studies raised the question of the relevance of pure geometrical markers for therapeutic decision making in evaluating the clinical relevance of vascular lesions. Computational fluid dynamics (CFD) has also been used for aortic haemodynamic analysis, particularly to obtain simulations of the blood flow behaviour in the abdominal aorta before and after stent-graft implantation [9, 10]. The purpose of this paper is to present a CFD method developed by a dedicated project to optimise the computational functional imaging of the arteries (OCFIA) and applied to achieve functional imaging of the thoracic aorta, particularly for those patients treated by stent-graft implantation.

Materials and methods

Three main phases characterise the method, as shown in Table 1: anatomical and haemodynamic acquisitions

(boundary conditions), static and dynamic geometry definition (native and moving meshes) and 4D simulations (CFD runs).

Acquisition protocol

Anatomical and functional data were obtained by 1.5 T MRI (Magnetom Avanto, Siemens, Erlangen, Germany) using two six-element body matrix coils. A standard protocol with contrast-enhanced MRA (CE MRA) of the thoracic aorta, cardiac-gated cine sequences and phase-contrast (PC) velocity mapping was used as follows: A breath-held, non-gated 3D-MRA was acquired after a test bolus injection of 2 ml gadoterate meglumine (Gd-DOTA, Dotarem®, Guerbet, Aulnay-Sous-Bois, France) to measure the arrival time of the bolus from injection in a cubital vein to the left atrium. After administration of 0.1 mmol/kg body weight Gd-DOTA at 2 ml/s followed by a saline chaser of 30 ml with the same injection rate, T1-fast field echo (FFE) sequences were acquired in oblique-sagittal orientation during breath-hold with the following parameters: TR/TE=3.8/1.37 ms; flip angle 35°; slice thickness 2 mm; field of view 420 mm; spatial resolution $0.97 \times 1.09 \times 4 \text{ mm}^3$. A cardiac-gated (triggered from the R wave of the ECG), cine-segmented turbo field echo sequence (TR/TE=3.2/1.55 ms; flip angle 30°; slice thickness 6 mm; field of view 320 mm; spatial resolution $2 \times 2.33 \times 6 \text{ mm}$) was then programmed using the same orientation of the MRA in order to cover the whole aortic volume. A total of 100 phases were acquired over a breath-hold interval (5 slices, 20 cardiac phases/slice), and usually 30 slices (600 cardiac phases) were sufficient to cover the whole aortic geometry.

Velocity mapping was obtained by 2D PC MR sequences, orthogonal to the vessel axis, located at the ascending (inlet), descending aorta, and supra-aortic vessels (outlets). A region of interest (ROI) defined the vascular area on the magnitude PC images to extract velocity data samples corresponding to phase information.

Data processing and geometry reconstruction

The native volume acquired by the 3D MRA was analysed and segmented using a commercial CFD mesh generator (Amira 4.1, TGS, Mercury Computer Systems, USA) in order to reconstruct the full arterial morphology. The level-set segmentation technique [11] was applied to generate the corresponding outer wall surface. For the implantation site, the in-stent surface was extracted. Once segmentation is validated, the geometry was reconstructed through a triangular surface mesh discretisation in order to obtain a three-dimensional volume grid based on tetrahedra (native mesh). This is classically used to perform virtual simulations of unsteady fluid in rigid models and of coupled fluid-structure interaction (FSI) computations [12]. Wall

Table 1 Methodological process: acquisition, post-processing, computational fluid dynamics (CFD) runs

	Phase	Technique
Acquisition	B.C.: geometry	MRA
	B.C.: wall movements	Cine imaging
	B.C.: inlet and outlet profiles	PC MRI
Post-processing (static and dynamic geometry definition)	Native mesh	CFD mesh generator
	Moving mesh	NLTF
Functional imaging	4D simulations	CFD runs (FV method)

B.C. Boundary conditions, *NLTF* non-linear transformation fields (see text), *FV* fluid volume

movements were imposed on the native grid according to the cardiac-gated cine imaging and generated the moving mesh [13].

CFD methodology and computer code

The flow simulations were performed using the finite volume (FV) method, as implemented in the AVBP 6.0 Navier-

Stokes solver (CERFACS, European Centre for Research and Advanced Training in Scientific Computation, Toulouse, France).

Computational mesh

The time-dependent functions (flow boundary conditions) were synchronised with the parietal motion and imposed in

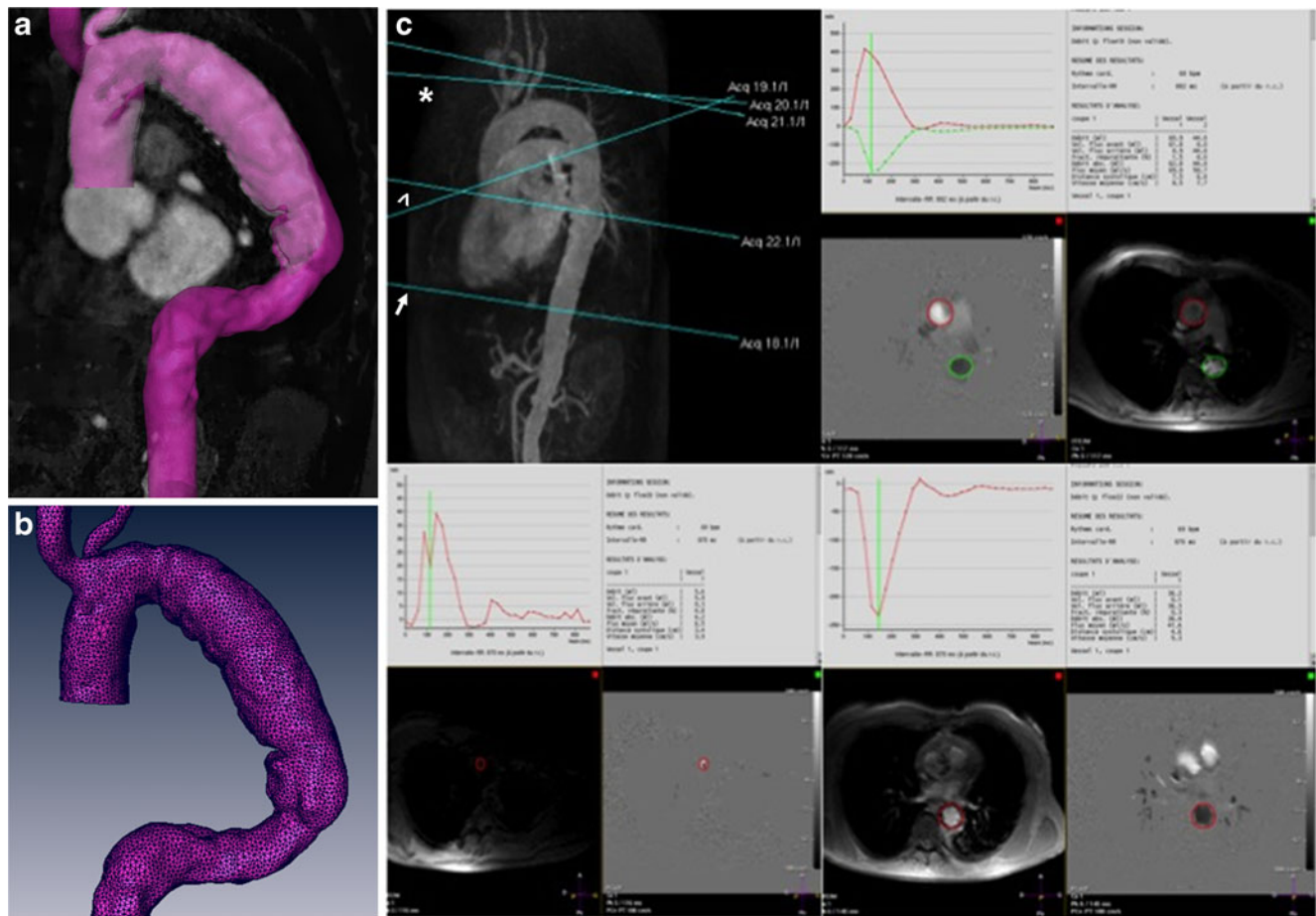


Fig. 1 **a** Boundary conditions, geometry: aortic morphology reconstruction was obtained by segmentation of the acquired volume using the level-set method (see text). **b** A tetrahedral grid (native mesh), exploitable for numerical calculations, was generated. Wall movements were imposed on this geometry according to the cine imaging (video 1 in the Electronic Supplementary Material). **c** Boundary conditions, haemodynamics: velocity mapping by PC MRI was performed at the

ascending (arrowhead) and descending aorta (arrow) and supra-aortic vessels (asterisk) to obtain inlet (ascending, above right) and outlet (supra-aortic vessels and distal descending, below) profiles defining haemodynamic conditions for computational fluid dynamics (CFD) calculations. Sequences were always acquired on a plane orthogonal to the vessel axis

the form of flow profiles at the entry (ascending aorta) and exit sections (descending aorta, supra-aortic vessels) of the numerical field (aortic district).

Blood was assumed to be a homogeneous Newtonian fluid with a dynamic viscosity approximated as 4 cP (valid for the main circulation) and a density of 1,050 kg/m³.

The FV method used in the code solves the full Navier-Stokes equation by an efficient explicit algebraic Lagrangian Eulerian (ALE) formulation, which allows the tetrahedral moving grid to be imposed within the cardiac cycles.

Results

Acquisitions

The total examination time for all MRI acquisitions was 25–35 min, depending on heart rate.

After in vitro validation [13], from October 2007 to January 2011, 20 patients (14 men; mean age 62.2 years) treated by thoracic endovascular aortic repair (TEVAR) for different lesions [seven thoracic aortic aneurysms (TAA), six dissections, two false aneurysms, two penetrating ulcers (PU), one intramural haematoma (IMH), and two acute traumatic aortic ruptures (ATAR)] were evaluated. Twenty post-operative controls using the described protocol were obtained. Two different devices were tested (Talent, Medtronic Vascular, Santa Rosa, CA; TAG, W.L. Gore, Flagstaff, AZ).

CFD imaging outcomes

Figure 1 illustrates surface generation and creation of the static tetrahedral mesh (the “native mesh”) containing the node coordinates, which could be read by the CFD software. A moving mesh was obtained by imposing wall movements on the native geometry according to the cine imaging, as shown in video 1 in the Electronic Supplementary Material (ESM).

After the CFD process, numerical results were compared with MRI for validation, as shown in Fig. 2, before launching 4D simulations. Dedicated visualisation software (Paraview Kitware, USA) was used to plot the blood flow modellings, depicting the aortic patterns of velocity and wall shear stress (WSS) by means of different modes and a colour-coded scale reported in meters per second (velocity) and Pascals (WSS). Blood flow visualisation included velocity vector graphs and 3D streamlines (at a tangent to the velocity field of an individual time frame), while WSS distribution was visualised by time-resolved particle traces.

Four-dimensional analysis of flow and WSS patterns was possible within the software package as the virtual models could be inspected from different view angles over the

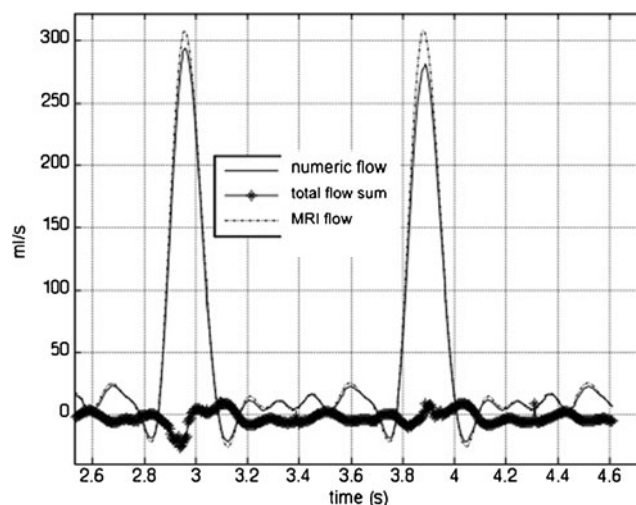


Fig. 2 Time-dependent function of the blood flow at the ascending aorta analysed by PC MRI and numerical calculation [computational fluid dynamics (CFD) results]. Comparison of the two techniques was used to validate the CFD results; the sum of the MRI and numerical measures should be null at any time

temporal dimension. Figure 3e (video 2 in the ESM) shows velocity imaging of post-TEVAR follow-up in a patient treated for type B aortic dissection extending from the arch to the abdominal aorta. When compared with the angiographic images, CFD imaging depicts by streamlines the flow behaviour and its magnitude all over the thoracic aorta, from ascending to in-stent lumen. Acceleration of the blood flow [peak systolic velocity (PSV), values >1.20 m/s and PSV ratio: stenosis/proximal vessel >2] is demonstrated in the narrowed vessel at the distal descending aorta, as expected from pathophysiology, where the true lumen is compressed by the false, and tortuous anatomy is present. Blood flow quality ranged from undisturbed, laminar patterns to complex or circular modes. Turbulent flow, depicted as “corkscrew”-type alterations, is highlighted in the distal descending aorta just above the narrowed segment, as shown in Fig. 3f.

WSS mapping of the same patient is shown in Fig. 4 (video 3 in the ESM), where localised WSS alterations are depicted at the arch and at the thoraco-abdominal transition. These areas correspond on the angiography to the proximal end of the stent-graft and to the distal, apparently moderate, narrowing of the distal descending aorta. A focal spot of increased WSS is further revealed along the inner wall of the descending aorta and was hypothesized to correspond to an in-fold of the stent-graft tissue.

Velocity mapping was obtained in a patient treated for a large contained rupture at the isthmic region. Figure 5c (see also video 4 in the ESM) shows localised in-stent flow accelerations corresponding to zones of sharp irregularities of the stent-graft profile, with PSV values exceeding 1 m/s. In any segment, exploration could be implemented by

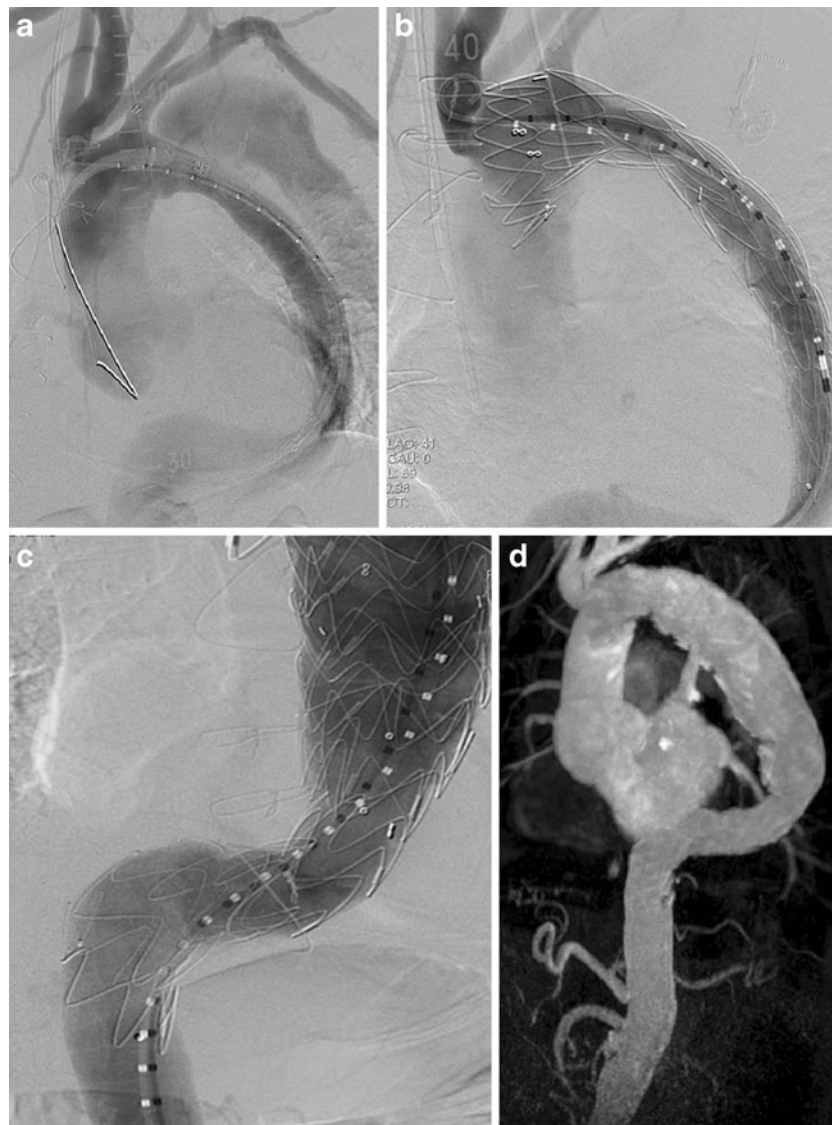


Fig. 3a–f Thoracic endovascular aortic repair (TEVAR) of a type B aortic dissection extending from the arch to the abdominal aorta. **a** Pre- and **b, c** post-implantation angiograms showing two stent-grafts placed from the arch, covering the left subclavian artery (LSA), to the distal descending aorta in order to treat different entry tears and the true lumen compression. **d** MRA and **e** velocity computational fluid dynamics (CFD) study at 1 year from the implantation: the true lumen is well

vector field analysis for further visual evaluation. Figure 5d (see also video 5 in the ESM) shows vector emitter planes placed normal to the longitudinal axis at the ascending aorta and arch. As expected from blood rheology in normal patterns, high velocity vectors are centrally located, occupying the majority of the vessel lumen, and with decreasing velocity approaching the vessel wall.

Figure 6 (see also videos 6a, b, c in the Electronic Supplementary Material) shows the instantaneous WSS distribution in this patient. Increased regions of shear stress are visualised at the bifurcation of the brachiocephalic trunk (BCT)-left common carotid (LCC), as expected, but also at

expanded at the proximal and middle descending aorta, while a smaller diameter is observed at the distal part of the vessel (video 2 in the Electronic Supplementary Material). Acceleration of blood flow is highlighted by red streamlines corresponding to >1.20 m/s velocity profiles, as indicated by the colour-coded scale (speed in meters per second). **f** Patterns of turbulent flow are depicted during different phases of the cardiac cycle just above the stenotic segment

the two zones of in-stent narrowing. Views from different angles could be obtained by freely rotating the virtual models (Fig. 6b, c) thus improving visual inspection of the WSS findings when compared to the CT images.

WSS mapping was obtained in a different patient treated for a TAA of the middle descending aorta (Fig. 7, video 7 in the ESM). Increased WSS spots were highlighted at the proximal and distal landing zones of the stent-graft when compared to the CT images. Distal alteration corresponds to a tortuous and narrowed segment, but no abnormal morphologic finding is evident at the proximal site.

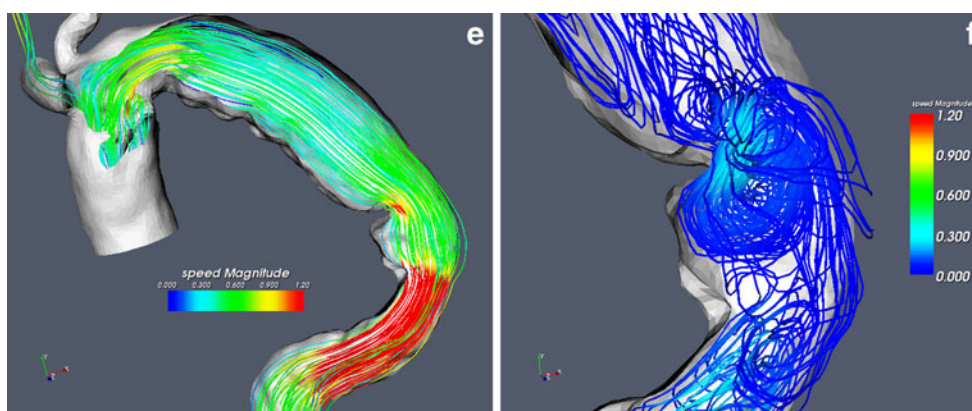


Fig. 3 (continued)

Discussion

The combination of magnetic resonance imaging and computational fluid dynamics offers an imaging method which provides haemodynamic imaging of the thoracic aorta in patients treated by stent-graft implantation. It has the potential to detect characteristics of locally altered flow, particularly of velocity and WSS, related to vascular lesions and stent configuration.

Evaluation of thoracic aorta has traditionally involved morphologic imaging techniques. However, just recently, time-resolved, 3D MRI at high-intensity field (3 T) has been proposed for the exploration of normal and pathological aortic vascular haemodynamics [4, 8, 14]. This approach suggests that functional changes rather than pure geometrical markers may be an important clinical marker for treatment planning, supporting other evidence about the relevance of characterising the dynamic components of

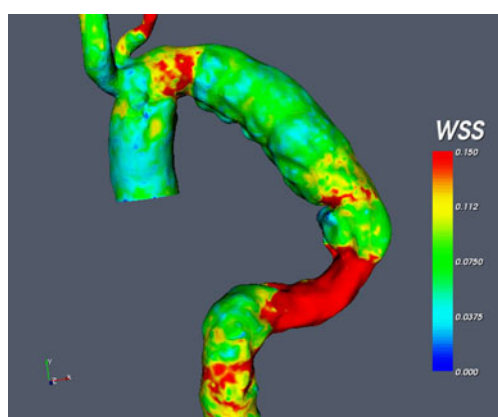
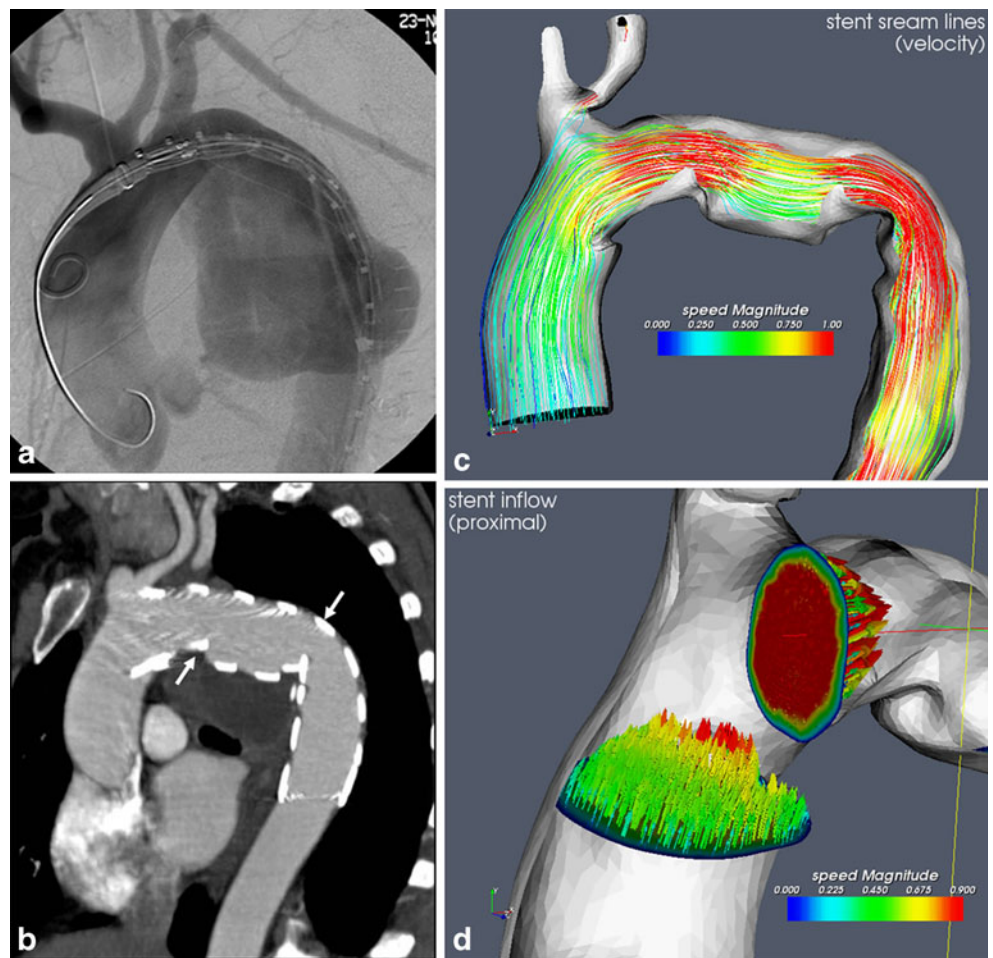


Fig. 4 Wall shear stress computational fluid dynamics (WSS-CFD) study of the patient in Fig. 3: localised alterations are depicted at the arch, corresponding to the proximal end of the stent-graft, and more distally along the narrowed portion, just above the thoraco-abdominal transition. A focal spot of increased WSS is further revealed along the inner wall of the descending aorta, possibly corresponding to an in-fold of the stent-graft tissue. See also video 3 in the Electronic Supplementary Material

blood flow to provide insights into normal and pathological physiology [15, 16]. Computational flow modelling has been used to analyse aortic haemodynamics initially after abdominal endovascular aortic repair (EVAR) [9, 10, 17]; more recently, functional assessments on thoracic endografts by CFD have been also reported [12, 18]. This paper presents the clinical application of a computational method dedicated to the evaluation of post-TEVAR aortic functional status. In our project, a 1.5 T MR machine is used for defining the boundary conditions; established protocol uses routine sequences with a total acquisition time similar to routine cardiac MR examinations. The use of MRI with MRA and cine imaging would provide more realistic geometric conditions which consider wall displacement over the cardiac cycle. Geometry extraction from the cine images would of course profit from an ECG-gated acquisition, but slice thickness (6–8 mm) would not be ideal for spatial definition. The extraction of the geometry was therefore realised on non-gated contrast-enhanced MRA. Motion artefacts on the MRA of the thoracic aorta with resultant blurring of the aortic walls have been described and can lead to inaccurate measurements at different levels of the thoracic aorta [19]. In our preliminary experience the geometry extracted by volume segmentation (native mesh) was visually inspected and compared to the cine imaging, as shown in video 1 in the ESM. The importance of clear MRI images to construct the geometry for realistic simulations has already been highlighted for the LV [20, 21], and the potential limits of blurring and ghosting artefacts in MRI due to breathing motion and bowel movement have been highlighted [20, 22]. To the best of our knowledge, no study has systematically evaluated the role of MRI to obtain geometry reconstruction of the anatomy of the thoracic aorta for flow modelling issues through CFD. Nevertheless Canstein et al. from the Freiburg group have described rapid prototyping model systems applied to MRA acquisitions for thoracic aorta modelling and subsequent haemodynamic analysis via CFD [14]. Larger experiences need to assess the reliability of the MRA for

Fig. 5a–d Thoracic endovascular aortic repair (TEVAR) for a large contained rupture at the isthmic region. **a** Intraoperative angiography and **b** post-operative CTA showing the stent-grafting of the aortic arch which involves the LSA origin. **c** Velocity-computational fluid dynamics (CFD) study demonstrates focal alterations of the flow velocity corresponding to the two zones of reduced in-stent diameter (*arrows*) (see also video 4 in the Electronic Supplementary Material). **d** Vector-field analysis performed at the proximal aortic arch from an emitter plane normal to the aortic axis, showing laminar distribution of the velocity vectors with maximum fields in the central lumen (see also video 5 in the Electronic Supplementary Material)



vascular geometry segmentation and the impact of the different artefacts on the aortic volume extraction.

All existing reports propose a static approach for flow modelling of aortic haemodynamics after stent-graft implantation. Haemodynamic variables were typical values for volumetric flow and pressure for the ascending aorta [12,

23], and pulsatile movement of the stent-grafts was assumed to be negligible [9]. The approach proposed in this paper imposes wall movements on the native mesh created by data processing and geometry reconstruction according to the fast cine sequences (video 8 in the ESM), thus reproducing more realistic conditions for the numerical simulations. Wall

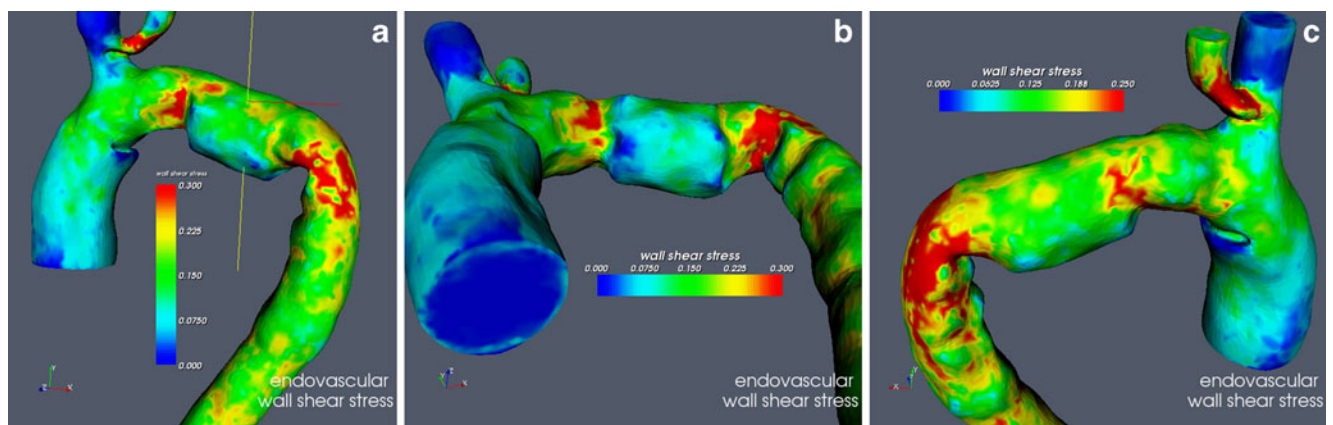


Fig. 6 Wall shear stress computational fluid dynamics (WSS-CFD) study of the patient in Fig. 5. Different views of the three-dimensional model depict focal spots of increased stress at two areas of stent-graft narrowing.

A third alteration is evident at the bifurcation of the brachiocephalic trunk (BCT)-left common carotid (LCC) as expected by vascular pathophysiology. See also video 6 in the Electronic Supplementary Material

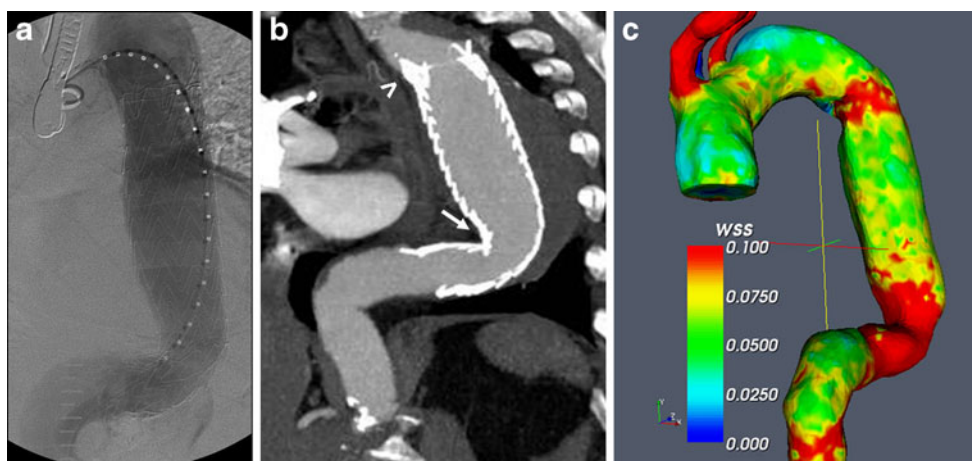


Fig. 7a–c Thoracic endovascular aortic repair (TEVAR) of the middle-descending aorta for a thoracic aortic aneurysm (TAA). **a** Intra-operative angiography and **b** CT control. **c** Post-implantation wall shear stress computational fluid dynamics (WSS-CFD) mapping showed increased fields of shear stress at the proximal and distal part of the stent-graft (see also video 7 in the Electronic Supplementary

Material). When compared with the morphologic studies, tortuosity (*arrow*) could explain the distal alterations, but no morphologic abnormal findings were found proximally (*arrowhead*). Nevertheless, the proximal spot seems to correspond to the proximal landing zone of the endograft

displacements of the numerical simulation over the cardiac cycle can clearly be observed in video 5 in the ESM. This could be a further step towards patient-specific computational flow modelling via a combination of MRI with CFD as already proposed for the left heart [21, 24]. In the first phase of our project, we focused our attention on velocity and WSS patterns. Haemodynamic patterns highlighted in Figs. 3e and 5f correspond to physiologic expectations in stenotic segments. Augmented PSV with linear flow patterns was found, even though complex helical flow has been demonstrated through a narrowed segment with 4D MRI evaluation of the thoracic aorta [8]. According to these authors, velocity sensitivity selection could be a determining factor to adjust image noise and avoid velocity aliasing. In our preliminary experience, a fixed velocity of 1.20 m/s was used for all examinations because no severe stenosis was expected. Nevertheless the expected physiologic patterns of laminar flow were demonstrated, as shown in vector field analysis of Fig. 5d, where maximum velocity fields appear in the central lumen.

The relevance of WSS study for clinical implications such as therapy monitoring or predicting parameters for vascular disease progression has already been postulated [25]. The role of displacement forces in endograft evolution has been investigated in *in vitro* and theoretical studies, and a connection with adverse events has been suggested [14]. The 3D modelling obtained after CFD runs provided panoramic anatomical maps of WSS distribution all over the thoracic aorta, as shown in Figs. 4, 6 and 7. The software package allowed detailed inspection by rotating and magnifying the images, thus enhancing comparative visual analysis with the morphologic CT or MR imaging. Local alterations of parietal stress were

outlined at expected zones of abnormal vascular geometry but also in correspondence with unsuspected regions where morphologic imaging did not enhance any pathologic finding, as shown in Fig. 7c at the proximal descending aorta. In the particular context of thoracic endovascular aortic repair, previous studies have analysed the influence of blood flow components on stent-graft implantation, suggesting that a deeper understanding of the forces experienced by the endograft may help to improve the performance and long-term durability of the devices [12, 18]. In accordance with our conclusions, these reports argued that new computational modelling techniques may improve our ability to identify endograft failure and may ultimately assist in future endograft designs, treatment planning and eventually in identifying new patient-specific prognostic factors. This paper presents the methodology of a novel approach, and it is not aimed at presenting clinical conclusions. Further studies are needed to assess the possible role of the method in clinical practice.

In conclusion, the computational method using the combined approach of magnetic resonance imaging and computational fluid dynamics for functional analysis of thoracic aorta after stent-graft implantation appears feasible. It seems to provide patient-specific assessments of the aortic haemodynamics with either panoramic mappings of blood flow patterns and local analysis of pathologic alterations. The dynamic approach to geometry definitions could be a step forward to more patient-specific analysis of the functional vascular status defining more realistic boundary conditions for flow modelling.

Further studies in the next phase of the project should evaluate specific clinical applications of the method in order to determine its potential to improve disease follow-up and treatment decisions.

Acknowledgements Ramiro Moreno has been financed during the development of the project by the Medtronic Vascular (Santa Rosa, CA); the project OCFIA has been supported by the French National Agency for Research (ANR 07-CIS7-006-01). CINES (Montpellier) is acknowledged for CFD calculations.

The early results of the project have been presented twice at the ECR, in 2008 and in 2011. The first presentation was honoured with the first prize in the vascular topic, of which we are sincerely proud.

References

- Fillinger MF, Greenberg RK, McKinsey JF, Chaikof EL (2010) Society for Vascular Surgery Ad Hoc Committee on TEVAR Reporting Standards. Reporting standards for thoracic endovascular aortic repair (TEVAR). *J Vasc Surg* 52:1022–1033
- Hodgson KJ, Matsumura JS, Ascher E, Dake MD, Sacks D, Krol K, Bersin RM, SVS/SIR/SCAI/SVMB Writing Committee (2006) Clinical competence statement on thoracic endovascular aortic repair (TEVAR)—multispecialty consensus recommendations. A report of the SVS/SIR/SCAI/SVMB Writing Committee to develop a clinical competence standard for TEVAR. *J Vasc Surg* 43:858–862
- Corbillon E, Bergeron P, Poullié AI, Primus C, Ojasoo T, Gay J (2008) The French National Authority for Health reports on thoracic stent grafts. *J Vasc Surg* 47:1099–1107
- Frydrychowicz A, Francois CJ, Turski PA (2011) Four-dimensional phase contrast magnetic resonance angiography: potential clinical applications. *Eur J Radiol* 80:24–35
- Hope TA, Herfkens RJ (2008) Imaging of the thoracic aorta with time-resolved three-dimensional phase-contrast MRI: a review. *Semin Thorac Cardiovasc Surg* 20:358–364
- Markl M, Draney MT, Miller DC et al (2005) Time-resolved three-dimensional magnetic resonance velocity mapping of aortic flow in healthy volunteers and patients after valve-sparing aortic root replacement. *J Thorac Cardiovasc Surg* 130:456–463
- Hope TA, Markl M, Wigstrom L, Alley MT, Miller DC, Herfkens RJ (2007) Comparison of flow patterns in ascending aortic aneurysms and volunteers using four-dimensional magnetic resonance velocity mapping. *J Magn Reson Imaging* 26:1471–1479
- Frydrychowicz A, Harloff A, Jung B et al (2007) Time-resolved, 3-dimensional magnetic resonance flow analysis at 3 T: visualization of normal and pathological aortic vascular hemodynamics. *J Comput Assist Tomogr* 31:9–15
- Howell BA, Kim T, Cheer A, Dwyer H, Saloner D, Chuter TA (2007) Computational fluid dynamics within bifurcated abdominal aortic stent-grafts. *J Endovasc Ther* 14:138–143
- Frauenfelder T, Lotfey M, Boehm T, Wildermuth S (2006) Computational fluid dynamics: hemodynamic changes in abdominal aortic aneurysm after stent-graft implantation. *Cardiovasc Intervent Radiol* 29:613–623
- Sethian JA (1999) Level set methods and fast marching methods: evolving interfaces in computational geometry, fluid mechanics, computer vision, and materials science, 2nd edn. Cambridge University Press, Cambridge
- Figueroa CA, Taylor CA, Chiou AJ, Yeh V, Zarins CK (2009) Magnitude and direction of pulsatile displacement forces acting on thoracic aortic endografts. *J Endovasc Ther* 16:350–358
- Moreno RNF, Veunac L, Rousseau H (2006) Non-linear-transformation-field to build moving meshes for patient specific blood flow simulations. In: Wesseling P, Onate E, Periaux J (eds) European conference on computational fluid dynamics. TU Delft, Delft
- Canstein C, Cachot P, Faust A et al (2008) 3D MR flow analysis in realistic rapid-prototyping model systems of the thoracic aorta: comparison with in vivo data and computational fluid dynamics in identical vessel geometries. *Magn Reson Med* 59:535–546
- Markl M, Harloff A, Bley TA et al (2007) Time-resolved 3D MR velocity mapping at 3 T: improved navigator-gated assessment of vascular anatomy and blood flow. *J Magn Reson Imaging* 25:824–831
- Lima JA, Desai MY (2004) Cardiovascular magnetic resonance imaging: current and emerging applications. *J Am Coll Cardiol* 44:1164–1171
- Molony DS, Kavanagh EG, Madhavan P, Walsh MT, McGloughlin TM (2010) A computational study of the magnitude and direction of migration forces in patient-specific abdominal aortic aneurysm stent-grafts. *Eur J Vasc Endovasc Surg* 40:332–339
- Prasad A, To LK, Gorrepati ML, Zarins CK, Figueroa CA (2011) Computational analysis of stresses acting on intermodular junctions in thoracic aortic endografts. *J Endovasc Ther* 18:559–568
- Srichai MB, Kim S, Axel L, Babb J, Hecht EM (2010) Non-gadolinium-enhanced 3-dimensional magnetic resonance angiography for the evaluation of thoracic aortic disease: a preliminary experience. *Tex Heart Inst J* 37:58–65
- Tay WB, Tseng YH, Lin LY, Tseng WY (2011) Towards patient-specific cardiovascular modeling system using the immersed boundary technique. *Biomed Eng Online* 10:52
- Saber NR, Gosman AD, Wood NB, Kilner PJ, Charrier CL, Firmin DN (2001) Computational flow modeling of the left ventricle based on in vivo MRI data: initial experience. *Ann Biomed Eng* 29:275–283
- Kitajima HD, Sundareswaran KS, Teisseyre TZ, et al (2008) Comparison of particle image velocimetry and phase contrast MRI in a patient-specific extracardiac total cavopulmonary connection. *J Biomech Eng* 130:041004
- Nichols WW, O'Rourke MF (2005) McDonald's blood flow in arteries: theoretical, experimental and clinical principles, 5th edn. Hodder Arnold, London
- Saber NR, Wood NB, Gosman AD et al (2003) Progress towards patient-specific computational flow modeling of the left heart via combination of magnetic resonance imaging with computational fluid dynamics. *Ann Biomed Eng* 31:42–52
- Wentzel JJ, Corti R, Fayad ZA, Wisdom P, Macaluso F, Winkelmann MO, Fuster V, Badimon JJ (2005) Does shear stress modulate both plaque progression and regression in the thoracic aorta? Human study using serial magnetic resonance imaging. *J Am Coll Cardiol* 45:846–854